LIMNOLOGY
and
OCEANOGRAPHY

ASLO

Limnol. Oceanogr. 63, 2018, 714–730

doi: 10.1002/lno.10662

Low and variable ecosystem calcification in a coral reef lagoon under natural acidification

Kathryn E. F. Shamberger [1,2*] **Steven J. Lentz** [2] **Anne L. Cohen** [2]
[1]Department of Oceanography, Texas A&M University, College Station, Texas
[2]Woods Hole Oceanographic Institution, Woods Hole, Massachusetts

Abstract

Laboratory-based CO_2 experiments and studies of naturally low pH coral reef ecosystems reveal negative impacts of ocean acidification on the calcifying communities that build coral reefs. Conversely, in Palau's low pH lagoons, coral cover is high, coral communities are diverse, and calcification rates of two reef-building corals exhibit no apparent sensitivity to the strong natural gradient in pH and aragonite saturation state (Ω_{ar}). We developed two methods to quantify rates of Net Ecosystem Calcification (NEC), the ecosystem-level balance between calcification and dissolution, in Risong Lagoon, where average daily pH is $\sim$ 7.9 and $\Omega_{ar} \sim 2.7$. While coral cover in the lagoon is within the range of other Pacific reefs ($\sim$ 26%), NEC rates were among the lowest measured, averaging 25.9 ± 13.7 mmol m^{-2} d^{-1} over two 4 d study periods. NEC rates were highly variable, ranging from a low of 13.7 mmol m^{-2} d^{-1} in March 2012 to a high of 40.3 mmol m^{-2} d^{-1} in November 2013, despite no significant changes in temperature, salinity, inorganic nutrients, Ω_{ar}, or pH. Our results indicate that the coral reef community of Risong Lagoon produces just enough calcium carbonate to maintain net positive calcification but comes dangerously close to net zero or negative NEC (net dissolution). Identifying the factors responsible for low NEC rates as well as the drivers of NEC variability in naturally low pH reef systems are key to predicting their futures under 21st century climate change.

Coral reefs are diverse marine ecosystems that support the livelihoods of hundreds of millions of people world-wide, protect thousands of kilometers of tropical coastline from waves, storms and tsunamis, and whose worth to the global economy is estimated in the trillions of dollars each year (Costanza et al. 2014). Many coral reefs today have been heavily and negatively affected by local human activities such as coastal development, overfishing, and pollution. In addition, ocean warming, acidification and rising sea levels caused by increasing anthropogenic carbon dioxide (CO_2) concentrations in the atmosphere present global scale threats from which no coral reef is immune.

Ocean acidification, the decline in global ocean pH caused by absorption of excess atmospheric CO_2, is of particular concern for tropical coral reefs due in large part to the coupled decline in seawater carbonate ion (CO_3^{2-}) needed to produce calcium carbonate ($CaCO_3$). The existence of coral reefs relies on $CaCO_3$ production by reef organisms, including corals and calcifying algae, to maintain the reef structure against erosion and dissolution. In experiments, the production of biogenic $CaCO_3$ generally decreases (e.g., Langdon et al. 2000, 2003), and bioerosion (e.g., Tribollet et al. 2009) and dissolution (e.g., Andersson et al. 2009) generally increase as pH decreases and availability of CO_3^{2-} is reduced. Taken together, these findings raise concerns that coral reefs could shift from net accreting to net eroding structures within the next few decades, compromising their ability to provide the ecosystem services upon which millions of people depend (Silverman et al. 2009).

Naturally low-pH coral reef systems are valuable natural laboratories to test hypotheses emerging from lab-based CO_2 manipulation experiments. Many low-pH reefs studied to date are characterized by reduced diversity, especially among calcifying organisms, reduced rates of coral calcification, and elevated rates of bioerosion (Manzello et al. 2008; Fabricius et al. 2011; Crook et al. 2012, 2013). Nevertheless, the effects of low pH and CO_3^{2-} concentration ($[CO_3^{2-}]$) on the coral reef communities of Palau are, for the most part, inconsistent with these findings. Here, coral diversity and richness increased and calcification rates of two massive reef-building genera, *Porites* and *Favia*, did not decline across a steep natural gradient in pH and $[CO_3^2]$ (Shamberger et al. 2014; Barkley et al. 2015). Further, in laboratory CO_2 manipulation

*Correspondence: katie.shamberger@tamu.edu

experiments, Palau *Porites* corals maintained calcification rates at pH as low as 7.5 (aragonite saturation state (Ω_{ar}) $\sim$ 1.3) revealing uncommon tolerance to low pH conditions when compared with *Porites* from other reefs (Barkley et al. 2017). Bioersion rates of *Porites* corals on Palau's low pH reefs are higher than they are on Palau's higher pH barrier reefs, but are still fairly low when compared with other reefs across the Pacific basin (DeCarlo et al. 2015). The apparent tolerance of Palau corals to low pH suggests that some corals could maintain rates of calcification conducive for reef-building under levels of acidification expected by the end of this century. Nevertheless, the overall $CaCO_3$ budget of the reef, which plays an important role in determining whether reefs grow or recede, is not determined solely by the calcification rates of individual coral colonies. Rather, the $CaCO_3$ budget is determined by rates of $CaCO_3$ production by all calcifiers in the community as well as rates of $CaCO_3$ loss to dissolution and transport by currents.

The impact of ocean acidification on $CaCO_3$ budgets is a primary concern yet it is difficult, if not impossible, to accurately assess the net $CaCO_3$ budget of a reef using individual measurements of calcification, dissolution, sediment fluxes, and erosion on the myriad different calcifying organisms that make up the community and/or blocks of $CaCO_3$. Over the last few decades, chemical methods have been developed and applied to quantify rates of Net Ecosystem Calcification (NEC) in coral reef environments. NEC is the balance between calcification and dissolution within a reef community, and provides a closer approximation of the $CaCO_3$ budget of the particular stretch of reef over which measurements are made than individual colony/block/sediment measurements. During NEC studies, data are often collected to concurrently enable quantification of Net Ecosystem Production (NEP), which is the reef scale balance between photosynthesis and respiration (e.g., Gattuso et al. 1996; Silverman et al. 2007; Shamberger et al. 2011; Albright et al. 2013; Silverman et al. 2014; Shaw et al. 2015; Bernstein et al. 2016; Muehllehner et al. 2016; DeCarlo et al. 2017). Several studies have identified seawater pH and Ω_{ar} as a dominant control of NEC, with NEC rates increasing as pH and Ω_{ar} increase (e.g., Shamberger et al. 2011; Albright et al. 2016). Silverman et al. (2009), using relationships derived from NEC measurements, predicted that NEC on reefs globally would fall below zero i.e., reefs would become net dissolving, around mid-century. However, both NEC and NEP influence seawater chemistry and it is difficult to disentangle the drivers from the responses. DeCarlo et al. (2017) compared average reef NEC of all studies conducted to date to Ω_{ar} of the source water to the reef and found no relationship, suggesting that other factors, in addition to pH, could play an important role in driving NEC rates. In addition, the pH and Ω_{ar} range over which studies have been conducted to date is relatively narrow. No NEC estimates have yet been derived for reefs under chronic natural acidification.

One reason for the narrow range of Ω_{ar} over which NEC studies have been conducted is that accurate estimates of NEC rates based on alkalinity anomaly techniques require reef conditions conducive to tracking a parcel of water across a reef and determining the residence time of that parcel on the reef. Previous NEC studies have generally been performed on coral reefs that experience either negligible water flow, often in restricted flow environments at low tide (slack water method, e.g., Ohde and van Woesik 1999; Shaw et al. 2012; Silverman et al. 2012), or unidirectional flow (flow respirometry methods: Lagrangian (e.g., Gattuso et al. 1996; Albright et al. 2013; Koweek et al. 2015) and Eulerian (e.g., Shamberger et al. 2011; Falter et al. 2012; Silverman et al. 2014; DeCarlo et al. 2017)) for some period of time, meaning that measurements can often only be made over several hours at a time. On Palau, low pH coral reef communities inhabit semi-enclosed lagoons with one or multiple channels connecting each lagoon to outer waters, resulting in complex, tidally driven flow regimes. This morphology makes the application of conventional alkalinity anomaly techniques challenging. For this reason, we developed two new methods to estimate coral reef NEC and NEP in a semi-enclosed lagoon using a combination of total alkalinity (TA), salinity, and volume budgets. We used this approach to quantify NEC and NEP in Palau's naturally low pH Risong Lagoon over four consecutive days in March 2012 and November 2013.

Methods

Study site

The Palauan archipelago is located in the western tropical Pacific spanning approximately 6.9–8.1°N and 134.1–134.7°E. The main islands of Palau are surrounded by an almost continuous barrier coral reef system that encompasses a large, protected lagoon hosting numerous islands and nearshore coral reefs. A series of uplifted karst islands, referred to as the Rock Islands, form a maze-like system of small bays and inlets in the southeastern part of the archipelago. Several of the Rock Island bays are characterized by persistently low pH and Ω_{ar} (average pH of 7.84–7.95 and average Ω_{ar} of 2.34–2.97), equivalent to conditions predicted to occur in the western tropical Pacific open ocean by the end of this century. This natural acidification is a result of the long residence time of water combined with the draw down of CO_3^{2-} and CO_2 production via net calcification, and CO_2 production via net respiration, i.e., community metabolism (Shamberger et al. 2014). Despite low pH and Ω_{ar}, coral cover in the bays is fairly high, as are coral genus diversity and richness, and calcification rates of two coral species do not decline significantly across the strong gradient in pH across the archipelago. Coral macrobioerosion rates are elevated compared to higher pH reefs in Palau but are not the highest

recorded in the Pacific (Barkley et al. 2015; DeCarlo et al. 2015).

This study investigates the NEC and NEP rates of Risong Lagoon within the Rock Islands (Fig. 1). Risong Lagoon is a small lagoon that is approximately 170 m long and 70 m wide and is connected to the larger Risong Bay by a single narrow channel approximately 28 m wide, 70 m long, and 0.8–2.2 m deep depending on tide (Fig. 1). The lagoon contains a coral reef ecosystem that forms a shallow (1–2 m depth) shelf along the walls of the lagoon. Live corals occur on top of the shelf and extend down the sides of the shelf to about 15 m depth and the lagoon floor is mud that has a maximum depth of approximately 22 m. Exchange between Risong Bay and Risong Lagoon is driven by the tide with bay surface water (0–2 m) entering the lagoon through the channel on the flood tide and lagoon surface water exiting through the channel on the ebb tide.

Study setup

In most coral reef systems, changes in TA reflect changes in calcification and dissolution of $CaCO_3$ only and can be used to calculate NEC, a method known as the alkalinity anomaly technique (Smith and Key 1975). NEP can be measured using changes in dissolved inorganic carbon (DIC) that are corrected for NEC and air-sea exchange of CO_2 (F_{CO2}). To determine NEC and NEP in Risong Lagoon, TA and DIC entering and leaving the lagoon through the channel were tracked over the full diel cycle using a combination of in situ instrumentation and discrete water sampling for two 4 d periods from 28-31 March 2012 (dry season) and 9-12 November 2013 (intermediate between wet and dry seasons). In addition, discrete water samples (TA, DIC, and salinity) were collected at 1 m, at least twice a day in Risong Bay (Fig. 1, site 1, water depth approximately 30 m), and every 2 h during the day in the center of the lagoon at 1 m and 3 m in March 2012 and at 1 m, 3 m, and 10 m in November 2013 (Fig. 1, site 5). Conductivity, temperature, and depth (CTD) casts were performed during collection of each discrete sample in 2012 with a RBR XR-620 CTD with manufacturer stated conductivity, temperature, and depth accuracies of ± 0.003 mS cm^{-1}, ± 0.002°C, and ± 0.05%, respectively, and in 2013 with a YSI Castaway CTD with manufacturer stated salinity, temperature, and depth accuracies of ± 0.1, ± 0.05°C, and ± 0.25%, respectively.

Three sites were established within the channel (Fig. 1, sites 2–4) to track water entering and leaving the lagoon. In March 2012, SeaBird SeaGauge sensors that measure pressure, temperature, and salinity were deployed at sites 2 and 4 and an Aquadopp Acoustic Doppler Profiler (ADP) current meter, Seabird microcat temperature and salinity sensor, and McLane Laboratories Remote Access Sampler (RAS) were deployed at site 4. In November 2013, SeaGauge sensors were deployed at sites 2–4 and an Aquadopp ADP, Seabird microcat, SAMI-pH sensor, Onset HOBO dissolved oxygen (DO) logger, and RAS were deployed at site 3 in the center of the channel. The ADP and RAS were moved from site 4 in 2012 to site 3 in 2013 to ensure water flowing through the channel was characterized. The RAS collected discrete water samples for TA and DIC analyses every 2 h from approximately 0.8 m (2012) or 0.5 m (2013) above the sea floor (*see* Shamberger et al. (2011) for details on utilizing a RAS to collect seawater carbonate chemistry samples). In addition, a mooring was deployed in the center of the lagoon (Fig. 1, site 5) with a Seabird microcat at 3 m depth in 2012 and with Seabird microcats at 1 m and 3 m depth and a SAMI-pH sensor and HOBO DO logger at 1 m depth in 2013. In November 2013, a Li-Cor LI-192 quantum sensor measured photosynthetically active radiation (PAR) at several sites within Risong Lagoon between approximately 11:45 and 15:00. Discrete samples (TA, DIC, salinity) collected at lagoon sites 3, 4, and 5 were used to correct RAS and SAMI-pH carbonate chemistry data and microcat salinity data for any offsets. Drift was not detected in any of the instrumentation data over either 4 d study.

Sampling in the lagoon in March 2012 indicated the presence of low salinity, high TA and DIC submarine groundwater discharge (SGD) that could potentially affect NEC and NEP calculations, depending on the magnitude of the flux of SGD to the lagoon. Therefore, sampling was performed in November 2013 to characterize the water chemistry of SGD and to quantify the flux of SGD into the lagoon. SGD in the lagoon was visible at site 6 (Fig. 1) at low tide as a small plume of freshwater mixing with seawater from a crack in the karst wall that was exposed at low tide. CTD casts were performed and discrete water samples were collected multiple times a day at site 6 for TA, DIC, barium (Ba), strontium (Sr), uranium (U), and salinity analyses. SGD TA and DIC were assumed to be the same in 2012 and 2013 when performing NEC and NEP calculations. In addition, TA, DIC, and trace metal (Ba, Sr, U) samples were collected at site 3 every hour during one outgoing tide in order to quantify SGD flux into the lagoon. Trace metal samples were also collected at site 1 in Risong Bay twice a day and at site 5 in the lagoon at least once a day.

Water sample collection and analyses

Discrete water samples were collected from a Niskin in most cases but in 2013 the thin surface layer (< 1 cm) of SGD water entering the lagoon during low tide at site 6 was sampled with a 500 mL glass syringe. Discrete samples collected at the RAS intake line during RAS sampling were also collected with the glass syringe in 2013. Niskin and syringe samples were immediately transferred into 300 mL (TA/DIC) and 125 mL (salinity) borosilicate glass bottles. Approximately 5 mL were removed from each bottle to allow headspace for expansion and each TA/DIC sample was poisoned with 50 μL saturated mercuric chloride solution immediately after collection to inhibit biological activity, and then sealed

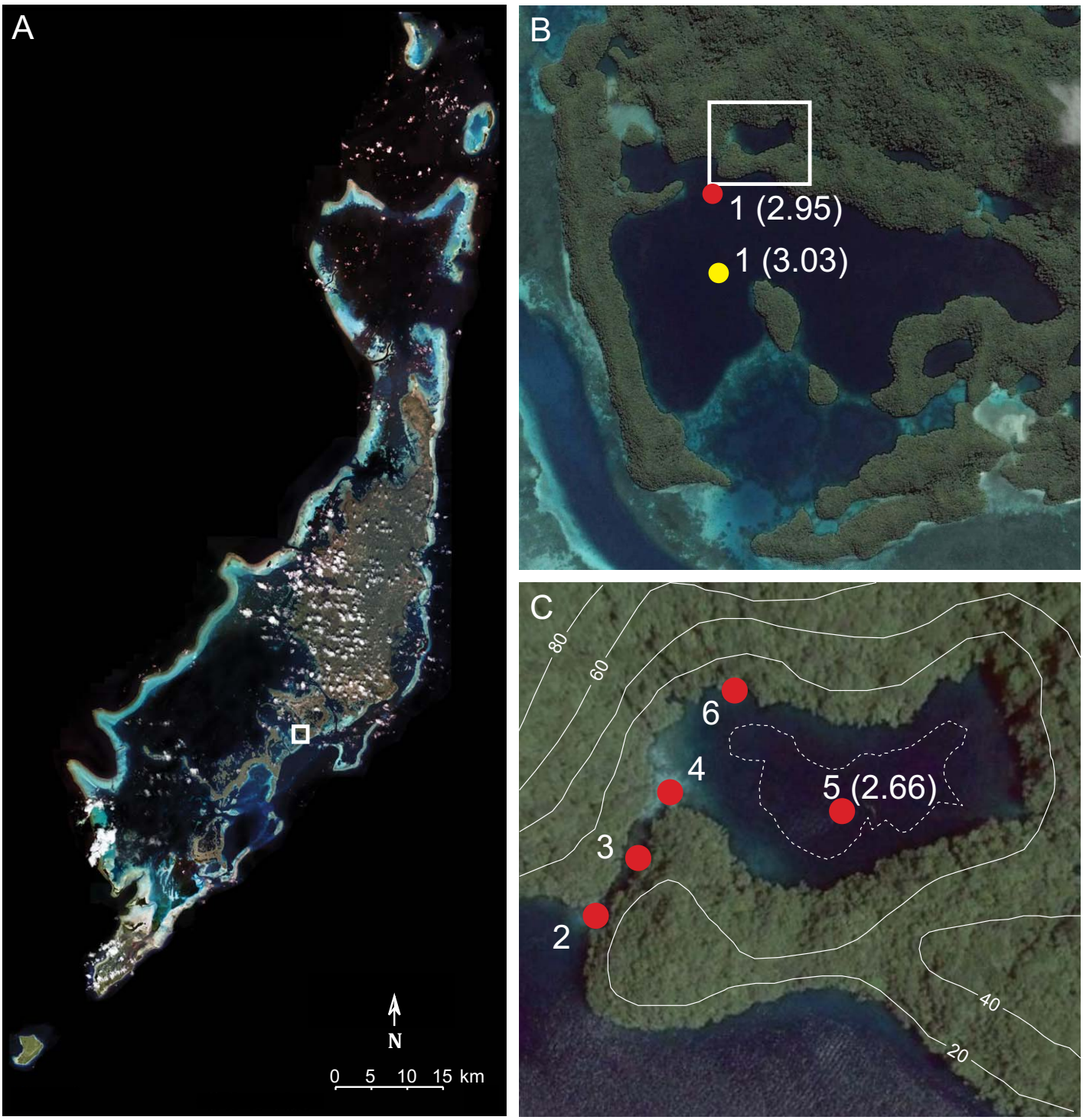

Fig. 1. Satellite images of Palau. IKONOS 4 m multispectral image provided by NOAA National Centers for Coastal Ocean Science, Silver Spring, Maryland, shows main islands of Palau (**A**) with white box around Risong Bay. Google Earth images show Risong Bay (**B**) with white box around Risong Lagoon (**C**). The dotted white line shows the extent of the reef with live coral in Risong Lagoon (**C**). The bottom of the lagoon inside the dotted white line has no live coral. Thin white lines represent topographic contours in meters (**C**). Circles show sampling locations with 1 m average aragonite saturation states in parentheses for select sites. Risong Bay (**B**) was sampled in different locations in March 2012 (yellow) and November 2013 (red).

with screw tops and tape. Water samples collected by the RAS were collected in pre-poisoned (200 μL mercuric chloride in $\sim$ 470 mL samples) Tedlar® or Kynar® bags obtained from McLane Research Laboratories and were immediately transferred to 300 mL borosilicate glass bottles following the 4 d deployments. SGD trace metal samples (Ba, Sr, U) were 0.2 μm filtered into clean LDPE bottles and acidified with nitric acid.

TA and DIC analyses were performed with a Versatile INstrument for the Determination of Total inorganic carbon and titration Alkalinity (VINDTA) produced by Marianda Marine Analytics and Data. The VINDTA uses coulometric titration for DIC analysis and an open cell potentiometric titration for TA analysis. DIC and TA measurements were standardized with certified reference materials obtained from Andrew Dickson at Scripps Institution of Oceanography (Dickson et al. 2007). Analyses of replicate samples yielded a mean precision of approximately ± 3 μmol kg^{-1} and ± 1.5 μmol kg^{-1} or better for DIC and TA analyses, respectively. Bottle salinity was measured on a Guildline Autosal salinometer.

Calculations

NEC and NEP rates were calculated using two different methods that combine TA, DIC, water volume, and salinity budgets for Risong Lagoon. The first method includes the entire volume of water within the lagoon (total volume method) and the second method includes only the lower layers of the lagoon below 2 m and hence excludes any freshwater influence (i.e., precipitation/evaporation, runoff, and SGD) on the NEC and NEP calculations (lower layer method). The influence of freshwater input into the lagoon on NEC and NEP calculations can therefore be evaluated by comparing the total volume and lower layer results.

Total volume calculations

Equations 1, 2 show the total volume TA and DIC budgets, respectively, for Risong Lagoon:

$$d\left(V^{\mathrm{RL}}\mathrm{TA}^{\mathrm{RL}}\right)/dt = \mathrm{TA}^{\mathrm{c}}u^{\mathrm{c}}h^{\mathrm{c}}W^{\mathrm{c}} - 2\mathrm{NEC}\left(A^{\mathrm{RL}}\right)/\rho + \mathrm{TA}^{\mathrm{SGD}}U^{\mathrm{SGD}} \quad (1)$$

$$\begin{aligned} d\left(V^{\mathrm{RL}}\mathrm{DIC}^{\mathrm{RL}}\right)/dt &= \mathrm{DIC}^{\mathrm{c}}u^{\mathrm{c}}h^{\mathrm{c}}W^{\mathrm{c}} \\ &- \left(\mathrm{NEC} + \mathrm{NEP} + F_{\mathrm{CO2}}\right)\left(A^{\mathrm{RL}}\right)/\rho + \mathrm{DIC}^{\mathrm{SGD}}\left(U^{\mathrm{SGD}}\right) \end{aligned} \quad (2)$$

where V^{RL} is the total volume of the lagoon (m^3); $\mathrm{TA}^{\mathrm{RL}}$ and $\mathrm{DIC}^{\mathrm{RL}}$ are depth averaged TA and DIC in the lagoon at site 5; TA^{c} and $\mathrm{DIC}^{\mathrm{c}}$ are TA and DIC in the channel at site 3 (2013) or 4 (2012); u^{c} is current velocity (cm s^{-1}) in the channel at site 3 (2013) or 4 (2012); h^{c} is the depth (m) of the channel; W^{c} is the width (m) of the channel; A^{RL} is the area of the lagoon (m^2); ρ is density (kg m^{-3}); $\mathrm{TA}^{\mathrm{SGD}}$ and $\mathrm{DIC}^{\mathrm{SGD}}$ are the TA and DIC of SGD water; and U^{SGD} is SGD transport into the lagoon. Equation 1 states that temporal changes in TA in the lagoon (term on left side of Eq. 1) are due to TA entering and leaving the lagoon through the channel (first term on right side of Eq. 1), NEC within the lagoon (second term, right side), and SGD entering the lagoon (last term, right side). Equation 2 states that temporal changes in DIC in the lagoon are due to NEP and F_{CO2} in addition to flux through the channel, NEC, and SGD. NEC is multiplied by 2 in Eq. 1 but not in Eq. 2 because for every one mole of $CaCO_3$ produced, two moles of TA and one mole of DIC are consumed.

Equation 3 shows the total water volume budget for Risong Lagoon. Conservation of volume requires that temporal changes in water volume in the lagoon (term on left side of Eq. 3) due to changes in sea level (term second to the left in Eq. 3) are equal to the flux of water through the channel (first term, right side Eq. 3), SGD input into the lagoon (second term, right side), and precipitation plus runoff minus evaporation (PE):

$$d\left(V^{\mathrm{RL}}\right)/dt = A^{\mathrm{RL}}d\left(\eta^{\mathrm{RL}}\right)/dt = u^{\mathrm{c}}h^{\mathrm{c}}W^{\mathrm{c}} + U^{\mathrm{SGD}} + bA^{\mathrm{RL}}\mathrm{PE} \quad (3)$$

where $d(\eta^{\mathrm{RL}})/dt$ is the time rate of change of sea level in the lagoon measured at site 4 and b is a multiplicative factor to account for runoff. The corresponding salt budget for the lagoon is:

$$d\left(S^{\mathrm{RL}}V^{\mathrm{RL}}\right)/dt = u^{\mathrm{c}}h^{\mathrm{c}}W^{\mathrm{c}}S^{\mathrm{c}} \quad (4)$$

where S^{RL} is the salinity of the lagoon at site 5 and S^{c} is salinity in the channel at site 3 (2013) or site 4 (2012). Assuming SGD salinity is zero and combining Eqs. 3, 4 gives Eq. 5 which states that temporal changes in salinity in the lagoon (term on left side of Eq. 5) are due to transport of salinity through the channel, SGD transport to the lagoon that lowers salinity, and precipitation plus runoff minus evaporation:

$$V^{\mathrm{RL}}d\left(S^{\mathrm{RL}}\right)/dt = \left(S^{\mathrm{c}} - S^{\mathrm{RL}}\right) * A^{\mathrm{RL}}d\left(\eta^{\mathrm{RL}}\right)/dt - S^{\mathrm{c}}\left(U^{\mathrm{SGD}} + bA^{\mathrm{RL}}\mathrm{PE}\right) \quad (5)$$

Thus, the total freshwater transport into the lagoon (F^{T}) from SGD and PE is:

$$\begin{aligned} F^{\mathrm{T}} = U^{\mathrm{SGD}} + bA^{\mathrm{RL}}\mathrm{PE} &= A^{\mathrm{RL}}d\left(\eta^{\mathrm{RL}}\right)/dt * \left(S^{\mathrm{c}} - S^{\mathrm{RL}}\right)/S^{\mathrm{c}} - V^{\mathrm{RL}}/S^{\mathrm{c}} \\ &* d\left(S^{\mathrm{RL}}\right)/dt \end{aligned} \quad (6)$$

Combining Eqs. 1, 3, and 6, and solving for NEC gives the following:

$$\begin{aligned} \mathrm{NEC} = (\rho/2)[&\left(\mathrm{TA}^{\mathrm{c}} - \mathrm{TA}^{\mathrm{RL}}\right)d\left(\eta^{\mathrm{RL}}\right)/dt - \mathrm{TA}^{\mathrm{c}}F^{\mathrm{T}}/A^{\mathrm{RL}} \\ &+ \mathrm{TA}^{\mathrm{SGD}}U^{\mathrm{SGD}}/A^{\mathrm{RL}} - h^{\mathrm{RL}}d\left(\mathrm{TA}^{\mathrm{RL}}\right)/dt] \end{aligned} \quad (7)$$

where h^{RL} is the average depth of the lagoon (13 m). Equation 7 states that NEC for the total volume of the lagoon can be calculated by accounting for advection of TA in and out of the lagoon through the channel (first term, right side of Eq. 7), greater transport of water out of the lagoon

through the channel than into the lagoon due to freshwater transport (precipitation/evaporation, runoff, and SGD) into the lagoon (second term, right side), an increase in TA due to SGD transport (third term, right side), and temporal changes in TA within the lagoon at site 5 (last term, right side). Positive NEC denotes net calcification while negative NEC denotes net dissolution of $CaCO_3$.

Similarly, combining Eqs. 2, 3, and 6, and solving for NEP gives the following:

$$\begin{aligned}\mathrm{NEP} = {} & \rho\left(\mathrm{DIC}^{c} - \mathrm{DIC}^{\mathrm{RL}}\right) d\left(\eta^{\mathrm{RL}}\right)/dt - \rho \mathrm{DIC}^{c} F^{\mathrm{T}}/A^{\mathrm{RL}} \\ & + \rho \mathrm{DIC}^{\mathrm{SGD}} U^{\mathrm{SGD}}/A^{\mathrm{RL}} - \rho h^{\mathrm{RL}} d\left(\mathrm{DIC}^{\mathrm{RL}}\right)/dt - \mathrm{NEC} - F_{\mathrm{CO2}}\end{aligned} \quad (8)$$

Equation 8 states that NEP for the total volume of the lagoon can be calculated by accounting for advection of DIC in and out of the channel, freshwater transport into the lagoon, an increase in DIC due to SGD, temporal changes in DIC within the lagoon, and corrections for NEC and F_{CO2}. Positive NEP denotes net photosynthesis while negative NEP denotes net respiration.

F_{CO2} depends on the gas transfer velocity (k), solubility of CO_2 as a function of salinity and temperature (s), and the difference between the partial pressure of CO_2 (pCO_2) in seawater (pCO_{2sw}) and air (pCO_{2air}) ($F_{CO2} = ks(pCO_{2sw} - pCO_{2air})$). Gas transfer velocity of the surface ocean is strongly affected by, and commonly parameterized with, wind speed. Wind speed is assumed to be zero in Risong Lagoon because it is completely surrounded and protected by steep slopes, which rise up to anywhere from 20 m to greater than 100 m height. Even under high wind conditions, waters within the lagoon are completely smooth and flat, limiting air-sea gas exchange. Previous work has shown that even under wind speeds as high as 7 m s^{-1} and ΔpCO_2 up to 210 μatm, F_{CO2} is an order of magnitude smaller than NEP in coral reef systems (Shamberger et al. 2011). Therefore, with negligible winds and an average ΔpCO_2 of 162 μatm in the lagoon, F_{CO2} is assumed to be negligible when calculating NEP.

The above NEC and NEP calculations (Eqs. 7, 8) assume that currents, TA, DIC, and salinity are spatially uniform in the channel.

Lower layer calculations

To exclude uncertainties associated with freshwater input, NEC and NEP were also calculated using budgets for the lower layers of the lagoon (below 2 m) by taking the difference between TA and DIC at 1 m in Risong Bay (site 1) and in the lagoon at 3 m and 10 m (site 5). These lower layer calculations exclude the influence of precipitation, runoff, evaporation, and SGD; assume there is no change in TA or DIC as water moves through the channel; and assume that surface (0–2 m) bay water entering the lagoon on the flood tide sinks into the lower layer and is distributed uniformly over the lower layer. Equations 9, 10 show the lower layer TA and DIC budgets for the lagoon, respectively:

$$V_L^{\mathrm{RL}} d\left(\mathrm{TA}_L^{\mathrm{RL}}\right)/dt = U^{\mathrm{F}}\mathrm{TA}^{\mathrm{RB}} - U^{\mathrm{F}}\mathrm{TA}_L^{\mathrm{RL}} - 2\mathrm{NEC}_L\left(A_L^{\mathrm{RL}}\right)/\rho \quad (9)$$

$$V_L^{\mathrm{RL}} d\left(\mathrm{DIC}_L^{\mathrm{RL}}\right)/dt = U^{\mathrm{F}}\mathrm{DIC}^{\mathrm{RB}} - U^{\mathrm{F}}\mathrm{DIC}_L^{\mathrm{RL}} - \left(\mathrm{NEC}_L + \mathrm{NEP}_L\right)\left(A_L^{\mathrm{RL}}\right)/\rho \quad (10)$$

where the subscript "L" indicates the lower layer of the lagoon below 2 m; U^{F} is average flood tide (only) volume transport through the channel calculated from current data in the channel; $\mathrm{TA}^{\mathrm{RB}}$ and $\mathrm{DIC}^{\mathrm{RB}}$ are the 4 d average TA and DIC of Risong Bay at 1 m at site 1; and $\mathrm{TA}_L^{\mathrm{RL}}$ and $\mathrm{DIC}_L^{\mathrm{RL}}$ are the 4 d average of the depth averaged (3 m and 10 m data) TA and DIC in the lagoon at site 5. Equation 9 states that temporal changes in TA in the lagoon below 2 m (term on left side of Eq. 10) are due to bay surface water entering the lagoon through the channel on the flood tide (first term on right side of Eq. 9), flux of TA from the lower layer into the upper layer of the lagoon (second term, right side), and NEC within the lagoon (third term, right side). Equation 10 states that temporal changes in DIC in the lagoon below 2 m are due to NEP in the lower layer in addition to transport from the bay through the channel, flux from the lower layer to upper layer, and NEC_L. Solving Eq. 9 for NEC_L and Eq. 10 for NEP_L gives the following:

$$\mathrm{NEC}_L = (\rho/2)\left[U^{\mathrm{F}}/A_L^{\mathrm{RL}}\left(\mathrm{TA}^{\mathrm{RB}} - \mathrm{TA}_L^{\mathrm{RL}}\right) - h_L^{\mathrm{RL}} d\left(\mathrm{TA}_L^{\mathrm{RL}}\right)/dt\right] \quad (11)$$

$$\mathrm{NEP}_L = \left(\rho U^{\mathrm{F}}/A_L^{\mathrm{RL}}\right)\left(\mathrm{DIC}^{\mathrm{RB}} - \mathrm{DIC}_L^{\mathrm{RL}}\right) - \rho h_L^{\mathrm{RL}} d\left(\mathrm{DIC}_L^{\mathrm{RL}}\right)/dt - \mathrm{NEC}_L \quad (12)$$

Equation 11 states that NEC in the lagoon below 2 m can be calculated by accounting for the flux of bay surface water TA into the lower layer of the lagoon on the flood tide and the flux of TA from the lower layer into the upper layer (first term, right side of Eq. 11), and temporal changes in TA in the lower layer of the lagoon (second term, right side). Equation 12 states that NEP for the lagoon below 2 m can be calculated by accounting for the flux of bay surface water DIC into the lower layer, flux of DIC from the lower layer into the upper layer, temporal changes in DIC in the lower layer, and correcting for NEC_L.

Carbonate chemistry calculations

The full seawater CO_2 system was calculated using in situ salinity, temperature, TA, and DIC data using an Excel Workbook Visual Basic for Applications translation of the original CO2SYS program (Lewis et al. 1998) by Pelletier, Lewis, and Wallace at the Washington State Department of Ecology, Olympia, Washington. The CO2SYS program was run with carbonate constants from Mehrbach et al. (1973) refit by Dickson and Millero (1987). All pH data presented were calculated on the total pH scale.

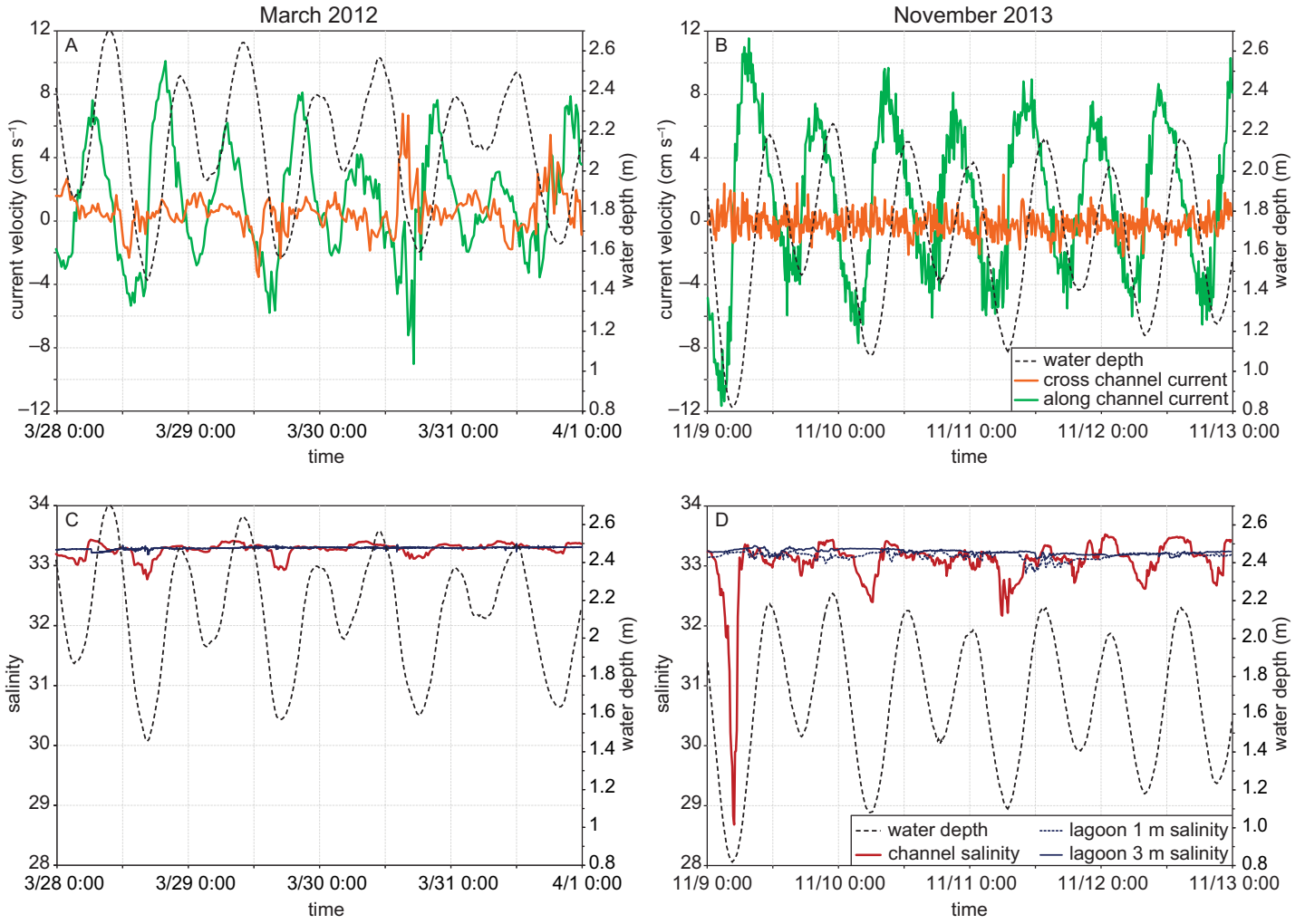

Fig. 2. Physical water parameters in the channel and lagoon of Risong Lagoon vs. time. Water depth (black dashed line), cross channel current velocity (orange line, positive velocities toward the northwest), and along channel current velocity (green line, positive velocities toward the lagoon) near the channel at site 4 (*see* Fig. 1 for site numbers) in March 2012 (**A**) and in the channel at site 3 in November 2013 (**B**). Water depth and salinity (red line) at site 4 and salinity at 3 m at site 5 (solid blue line) in March 2012 (**C**), and water depth and salinity in the channel and salinity at 1 m (dotted blue line) and 3 m at site 5 in November 2013 (**D**).

Ecological survey

Ecological surveys were performed in Risong Lagoon in January 2015 by the Palau International Coral Reef Center (PICRC). Eight 50 m transects were laid at 3 m depth and seven 50 m transects were laid at 10 m depth around the entire circumference of the lagoon, with a few meters between each transect. For each transect, a photograph was taken at every meter, resulting in 50 photographs per transect. The photographs were analyzed using Coral Point Count with Excel extensions (CPCe) (Kohler and Gill 2006) to the genus level for corals. Five random points from each quadrat were used to determine percent cover. Data from the 50 quadrats were averaged to provide the mean for each transect and the eight transects at 3 m were averaged and the seven transects at 10 m were averaged to provide the mean for each depth. In addition, divers surveyed the distance the reef extends from the karst walls toward the center of the lagoon by slowly swimming the circumference of the lagoon at the maximum depth of live corals while towing a float with a GPS that recorded latitude and longitude every 10 s (Fig. 1C).

Results

Hydrodynamics

Exchange between Risong Bay and Risong Lagoon is driven by tidal flow in the channel and along channel currents dominate with speeds up to 12 cm s^{-1} while cross channel currents are generally less than 2 cm s^{-1} (Fig. 2). Current velocity data at site 4 in 2012 are primarily

representative of channel transport although there is more variability in the cross channel current velocities than at site 3 in the center of the channel (Fig. 2). The water depth range over the 4 d studies was approximately 1.4–2.7 m at site 4 in 2012 and 0.8–2.2 m at site 3 in 2013 (Fig. 2).

The influence of fresh water input (precipitation, runoff, and SGD) in the lagoon is limited to the top 2 m of the water column (Fig. 3). CTD casts in the center of the lagoon measured salinity as low as 32 at 0.15 m, the shallowest depth resolved by the CTD (Fig. 3). In addition, in the center of the channel, salinities approaching 32 were detected at low tide when outgoing lagoon surface water was sampled at less than 0.3 m depth, and salinity as low as 28.2 was detected at approximately 5 cm depth, indicating a thin, lower salinity surface layer in the lagoon (Fig. 2D). Below approximately 2 m depth, lagoon salinity is stable and vertically uniform (Fig. 3). Continuous salinity data collected at site 5 at 1 m averaged 33.2 ± 0.1 (data presented as mean ± standard deviation throughout) in 2013 and at 3 m averaged 33.3 ± 0.1 in 2012 and 33.2 ± 0.04 in 2013 (Fig. 2B,D). Bay surface water has the same temperature, but consistently higher salinity and density than lagoon surface water (0.1–0.3 higher salinity in the bay on average) (Table 1; Figs. 2, 3). Bay surface water therefore sinks below 2 m when entering the lagoon on the flood tide and lagoon salinity below 2 m is consistent with average bay surface water (0–2 m) salinity (Fig. 3).

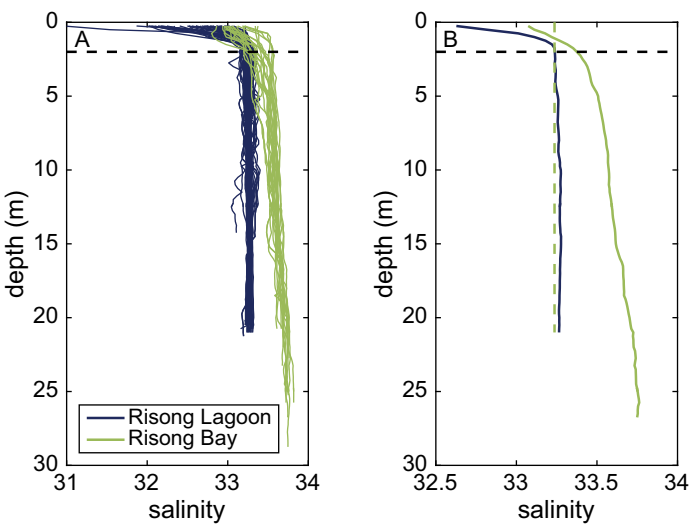

Fig. 3. Risong Bay and Lagoon salinity vs. depth profiles. (**A**) All salinity profiles measured at site 1 in Risong Bay (green lines) and site 5 in Risong Lagoon (blue lines) in November 2013. (**B**) The average of November 2013 Risong Bay (solid green line) and Risong Lagoon (solid blue line) salinity profiles and average salinity from 0 m to 2 m depth in Risong Bay (vertical dashed green line). Horizontal black dashed lines represent 2 m depth.

Water chemistry

Bay surface water has higher TA, pH, Ω_{ar}, and DO; and lower pCO_2, than lagoon surface water (Table 1). While daytime bottle data show lower surface water DIC on average in the bay compared to the lagoon (Table 1), data collected throughout the diel cycle show comparable surface water DIC levels in the bay and lagoon (Fig. 4). A diel cycle in TA is not evident in the bay or lagoon but there is a pronounced diel cycle in DIC (Fig. 4) and less pronounced, but detectable, diel cycles in pCO_2, pH, Ω_{ar}, and DO in both the bay (no DO data for the bay) and lagoon. DIC and pCO_2 are lower during the day and higher at night; pH, Ω_{ar}, and DO are higher during the day and lower at night; and the magnitude of these diel cycles is comparable in the bay and lagoon (Fig. 4). Continuous pH data collected at 1 m at site 5 in 2013 were corrected for an offset from pH calculated from TA and DIC bottle samples collected at the same time and depth by subtracting the average offset (0.012 ± 0.016) from the SAMI-pH measurements. Corrected, continuous pH data at site 5 in 2013 ranged from 7.85 to 7.92 and averaged 7.88 ± 0.01 (Fig. 5B). TA and DIC were lower in 2012 than in 2013 in the bay at 1 m, and in the lagoon at 1 m and 3 m (10 m samples were not collected in 2012). However, the mean TA/DIC ratio and therefore pH, pCO_2, and Ω_{ar}, are

Table 1. Average ± 1 standard deviation water chemistry data from discrete samples collected in Risong Bay (RB, site 1), Risong Lagoon (RL, site 5), and the channel connecting the bay and lagoon in March 2012 (site 4) and November 2013 (site 3).

Site	Year	Temp (°C)	Salinity	TA (μmol kg^{-1})	DIC (μmol kg^{-1})	pH	pCO_2 (μatm)	Ω_{ar}
RB	2012	30.0 ± 0.4	33.4 ± 0.0	2090.1 ± 4.3	1829.5 ± 8.3	7.95 ± 0.01	470 ± 15	3.03 ± 0.07
	2013	29.9 ± 0.3	33.2 ± 0.2	2109.5 ± 9.5	1857.5 ± 10.0	7.94 ± 0.01	490 ± 20	2.95 ± 0.11
Channel	2012	30.1 ± 0.3	33.3 ± 0.1	2061.8 ± 17.3	1850.8 ± 13.2	7.85 ± 0.04	600 ± 62	2.51 ± 0.17
	2013	29.9 ± 0.3	33.1 ± 0.4	2096.2 ± 14.6	1867.8 ± 14.3	7.90 ± 0.04	550 ± 58	2.71 ± 0.21
RL 1 m	2012	30.2 ± 0.3	33.1 ± 0.2	2065.4 ± 3.9	1840.9 ± 11.8	7.88 ± 0.02	560 ± 31	2.66 ± 0.11
	2013	30.3 ± 0.2	33.0 ± 0.2	2084.5 ± 6.1	1862.2 ± 11.3	7.88 ± 0.02	570 ± 28	2.65 ± 0.08
RL 3 m	2012	30.2 ± 0.2	33.3 ± 0.0	2062.2 ± 3.7	1831.2 ± 8.5	7.89 ± 0.02	530 ± 26	2.71 ± 0.09
	2013	30.2 ± 0.1	33.2 ± 0.2	2081.4 ± 4.8	1853.5 ± 5.5	7.89 ± 0.01	550 ± 11	2.69 ± 0.04
RL 10 m	2013	30.0 ± 0.1	33.3 ± 0.2	2091.5 ± 3.6	1859.3 ± 4.4	7.90 ± 0.01	540 ± 16	2.74 ± 0.06

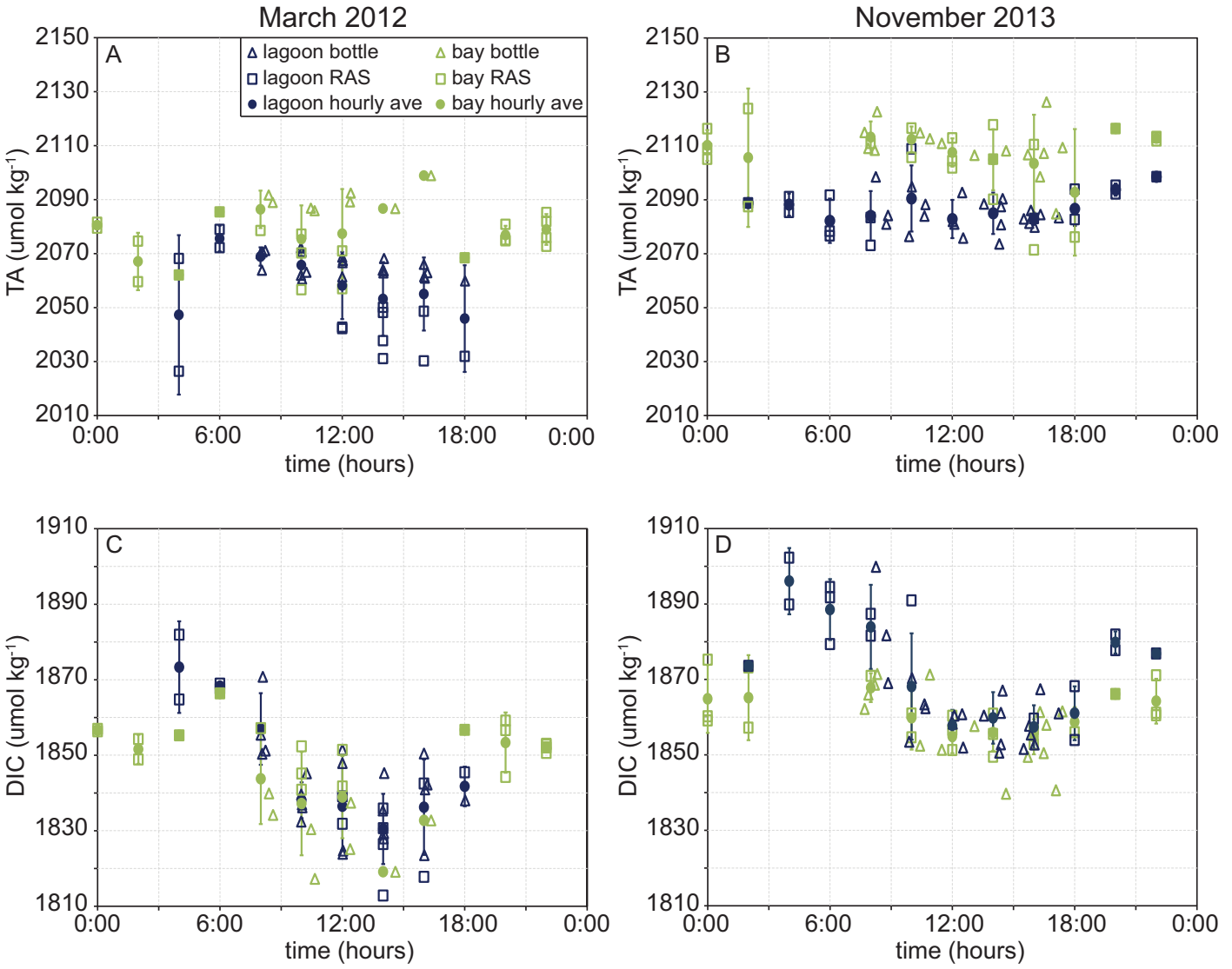

Fig. 4. Risong Bay and Lagoon carbonate chemistry diel cycles. Total alkalinity (TA, **A**, **B**) and dissolved inorganic carbon (DIC, **C**, **D**) collected in March 2012 (**A**, **C**) and November 2013 (**B**, **D**) in Risong Lagoon (dark blue symbols) and Risong Bay (green symbols) using discrete bottles (open triangles) and a Remote Access Sampler (RAS, open squares). RAS data were separated into either bay or lagoon water based on tides and water chemistry. Hourly averages ± one standard deviation are shown in closed circles with error bars.

statistically indistinguishable between the two sampling periods (Table 1; Fig. 4).

Water chemistry in the channel followed the tides and cycled between bay surface water during flood tide and lagoon surface water during ebb tide (Figs. 2, 5). Continuous pH data collected in the channel in 2013 were corrected for an offset from pH calculated from TA and DIC bottle samples by subtracting the average offset (0.019 ± 0.008) from the SAMI-pH measurements. The difference between bay and lagoon surface water chemistry is larger than the magnitude of the diel cycles, making variability larger in the channel than in the bay or lagoon (Table 1; Fig. 5). For example, while the means of the 2013 continuous pH data are comparable in the channel and within the lagoon (channel = 7.89 ± 0.04; lagoon = 7.88 ± 0.01) the pH range in the channel (0.15) was double that within the lagoon (0.07) (Fig. 5). Similarly, means of the 2013 continuous DO data are comparable in the channel and lagoon (channel = 6.8 ± 0.6 mg L^{-1}; lagoon = 6.7 ± 0.3 mg L^{-1}) but the range of DO was larger in the channel than in the lagoon (channel = 3.0 mg L^{-1}; lagoon = 2.4 mg L^{-1}). However, a diel cycle in channel DIC, pH, and DO is discernable, superimposed on the tidal cycle, with lower DIC, and higher DO and pH, during the day and vice versa at night (Fig. 5).

Surface waters in Risong Bay have higher salinity, density, and TA than surface waters in Risong Lagoon. When bay

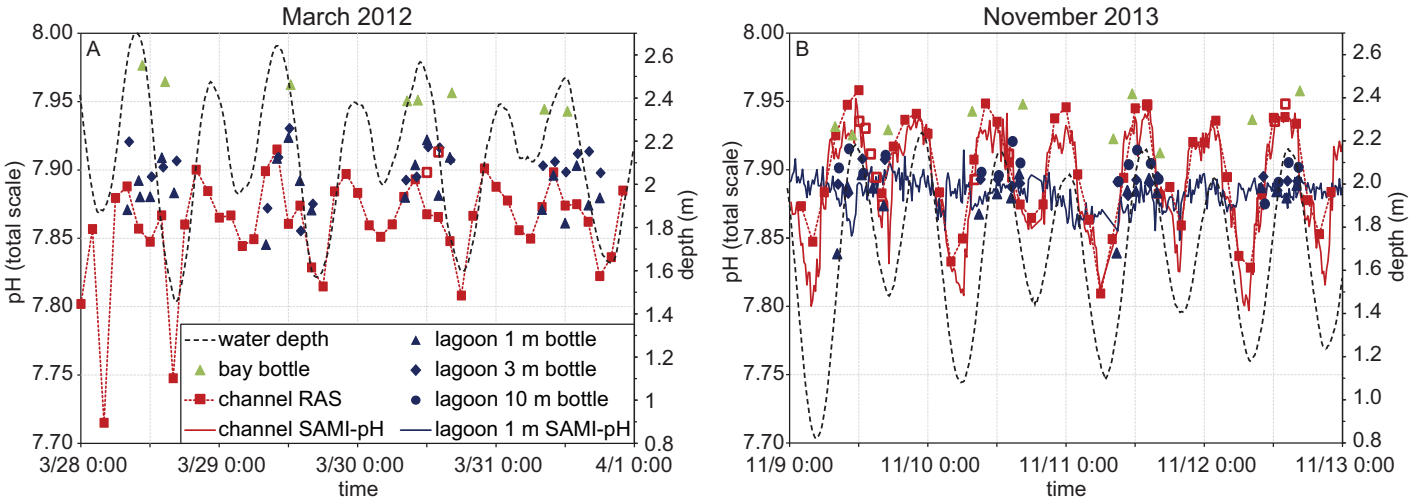

Fig. 5. Risong Bay and Lagoon pH vs. time. Data were collected in March 2012 (**A**) and November 2013 (**B**) in the channel connecting Risong Bay and Lagoon (site 4 in 2012, site 3 in 2013) by a Remote Access Sampler (RAS, red squares with dotted red line) and SAMI-pH (red solid line, 2013 only); in the center of Risong Lagoon (site 5) by discrete bottles at 1 m (blue triangles), 3 m (blue diamonds), and 10 m (blue circles, 2013 only) and SAMI-pH at 1 m (blue solid line, 2013 only); and in Risong bay (site 1) by discrete bottles at 1 m (green triangles). Dashed black lines show water depth at site 4 in 2012 and site 3 in 2013.

surface water enters the lagoon on the flood tide it sinks below 2 m and replaces surface water that flows out of the lagoon on the ebb tide. As a consequence of this exchange flow, the lower layer of the lagoon (below 2 m) is filled with surface water from Risong Bay and consequently has the same salinity. However, lagoon lower layer TA is less than bay surface water TA because calcification in the lagoon draws down TA. Lagoon TA reaches an equilibrium when the net flux of TA into the lagoon (the difference between bay surface water TA flowing in and lagoon surface water TA flowing out) equals the TA removed from lagoon water by calcification. Flushing time estimates based on the volume of the lagoon and the tidal flux in and out of the lagoon indicate that it takes approximately 1 (spring tides) to 2 (neap tides) weeks for the lagoon to reach equilibrium.

Submarine groundwater discharge

Elevated TA (up to 2570 μmol kg^{-1} at a salinity of 19.8) and DIC (up to 2560 μmol kg^{-1} at a salinity of 19.8) levels were measured in 2013 where SGD entered the lagoon at site 6 (Fig. 6A), but high TA and DIC were only detectable at low tide. Extending a linear least squares fit through all samples collected at site 6 to zero salinity gives an estimate of the TA and DIC of pure, zero salinity SGD water of approximately 3330 μmol kg^{-1} and 3600 μmol kg^{-1}, respectively. These zero salinity intercepts are consistent with a single freshwater sample collected from water dripping directly off the karst in the lagoon with a TA of 3420 μmol kg^{-1} and DIC of 3490 μmol kg^{-1} (Fig. 6A). Evidence of high TA SGD input in the lagoon can also be seen in the 1 m data at site 5 that show TA increasing slightly with decreasing salinity (Fig. 6B). In contrast, TA data at 1 m in the bay and at 3 m at site 5 fall along dilution lines and decrease with decreasing salinity, indicating no influence of increased TA from SGD (Fig. 6B). TA data at 10 m at site 5 in the lagoon have intermediate TA, between 1 m bay and 3 m lagoon levels, and a fairly constant salinity.

Trace metal concentrations were not elevated in any of the samples collected at site 6 or in the sample of freshwater dripping off the karst and therefore could not be used to track SGD flux into the lagoon. Therefore, a salinity budget (Eq. 6) was used to estimate freshwater transport into the lagoon from precipitation/evaporation, runoff, and SGD combined, of approximately 432 m^3 d^{-1}. To assess the influence of SGD on NEC and NEP calculations, total volume NEC and NEP estimates have been bounded by assuming all freshwater flux into the lagoon is either zero TA and DIC precipitation/runoff (lower bound) or high TA and DIC SGD (upper bound).

Net ecosystem calcification and production

Total volume and lower layer lagoon NEC estimates are positive (net calcification) and agree well for both years, with lower layer estimates falling within the range of total volume estimates, for both sampling periods (March 2012 NEC = 13.7–18.3 (total volume) and 16.2 (lower layer) mmol m^{-2} d^{-1}; November 2013 NEC = 31.4–40.3 (total volume) and 35.6 (lower layer) mmol m^{-2} d^{-1}; Table 2). Agreement between the total volume and lower layer NEC estimates, and the fact that the freshwater transport and SGD terms in the total volume NEC calculation are small, indicate that freshwater input, via precipitation/evaporation, runoff, and SGD, has a minimal impact on NEC calculations (Table 2). November 2013 NEC estimates are approximately twice

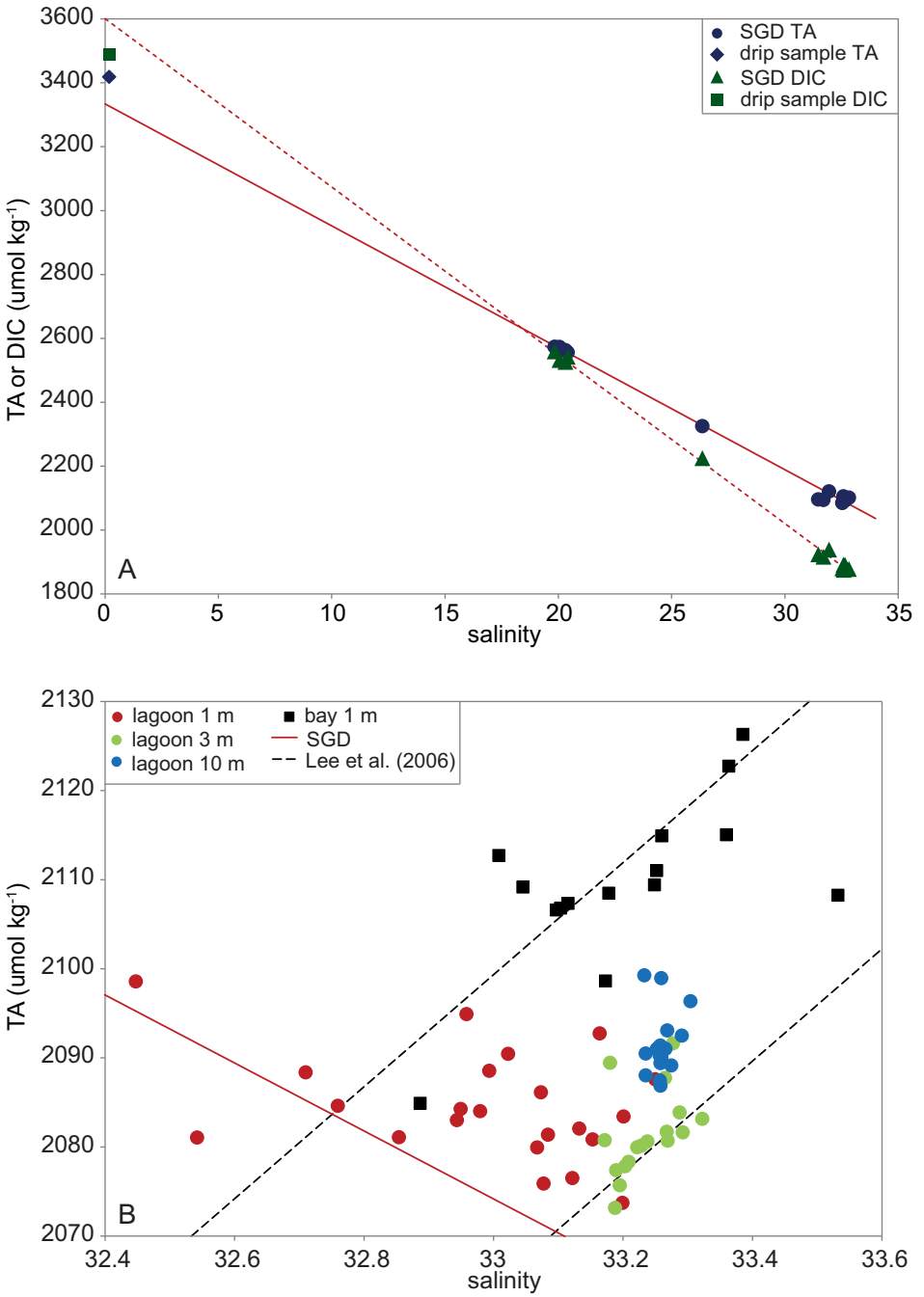

Fig. 6. Risong Bay and Lagoon carbonate chemistry vs. salinity in November 2013. (**A**) Total Alkalinity (TA; dark blue circles) and dissolved inorganic carbon (DIC; dark green triangles) vs. salinity (S) at site 6 where submarine groundwater discharge (SGD) entered Risong lagoon; linear least squares fit for TA vs. S at site 6 (solid red line: $TA = -38.17(S) + 3333.9$, $R^2 = 0.995$); linear least squares fit for DIC vs. S at site 6 (dotted red line: $DIC = -52.69(S) + 3600.9$, $R^2 = 0.998$); and TA (dark blue diamond) and DIC (dark green square) of freshwater dripping directly off the karst in Risong lagoon. (**B**) TA vs. S at 1 m (red circles), 3 m (green circles), and 10 m (light blue circles) at site 5 in Risong Lagoon and 1 m at site 1 in Risong Bay (black squares); TA vs. S trendline from (**A**) for site 6 data (red line); and TA dilution lines for the tropical Pacific open ocean from Lee et al. (2006) (dashed black lines).

those for March 2012, due to a large difference in the time trend term, which is small in 2012 and large in 2013 (Table 2). The 2012 NEC total volume and lower layer time trends are not significantly different from zero but the 2013 NEC time trend terms are significantly different from zero (2013 dTA/dt: total volume $= -2.5 \pm 1.2$ μmol kg^{-1} d^{-1}; lower layer 3 m data $= -3.3 \pm 1.4$ μmol kg^{-1} d^{-1} and 10 m data $= -1.9 \pm 1.4$ μmol kg^{-1} d^{-1}) and have high correlations

Table 2. Net ecosystem calcification (NEC) and production (NEP) in Risong Lagoon, calculated for the entire lagoon (total volume) and below 2 m depth (lower layer) in March 2012 and November 2013. The individual terms that contribute to the NEC and NEP calculations (advection, time trends (*d*TA/*dt* and *d*DIC/*dt*), freshwater transport, and submarine groundwater discharge (SGD)) are included (*see* Eqs. 7, 8, 12, 13). Total volume lower bounds assume all freshwater entering the lagoon is zero TA precipitation and runoff, and upper bounds assume all freshwater entering the lagoon is high TA SGD.

	March 2012		November 2013	
	Total volume	**Lower layer**	**Total volume**	**Lower layer**
NEC terms (mmol m^{-2} d^{-1})				
Advection	20.5	20.5	20.2	25.0
*d*TA/*dt*	−4.0	−4.3	16.8	10.6
Freshwater transport	−2.8	-	−5.6	-
SGD	4.6	-	8.9	-
Total NEC	13.7 to 18.3	16.2	31.4 to 40.3	35.6
NEP terms (mmol m^{-2} d^{-1})				
Advection	21.9	−2.9	11.0	9.3
*d*DIC/*dt*	11.5	8.1	15.0	−0.1
Freshwater transport	−5.0	-	−10.0	-
SGD	9.8	-	19.2	-
Total NEP	14.7 to 20.0	−11.0	−15.5 to −5.2	−26.4

between TA and time (total volume correlation = −0.76; lower layer 3 m correlation = −0.79 and 10 m correlation = −0.60). The advection, freshwater transport, and SGD NEC terms are approximately the same in 2012 and 2013 (Table 2).

In contrast to the NEC estimates, total volume and lower layer NEP estimates do not agree well for either sampling period (Table 2). In March 2012, total volume NEP is positive, indicating net photosynthesis, while lower layer NEP is negative, indicating net respiration. Lower layer and total volume NEP estimates are both negative in November 2013, but lower layer NEP is approximately twice the total volume lower estimate (Table 2). There are large discrepancies between the NEP total volume and lower layer advection (March 2012) and time trend (November 2013) terms and the NEP SGD term is twice the NEC SGD term.

Ecological survey

The coral reef community in Risong Lagoon is dominated by hard coral with cover averaging 22.4% ± 3.9% at 3 m and 53.0% ± 2.3% at 10 m (Table 3). Cover of macroalgae, crustose coralline algae, and invertebrates other than coral are low (< 6%) and no soft coral or seagrass were identified in any of the transects at either depth. Turf algae was abundant at 3 m (25.6% ± 4.7%) but not at 10 m (2.8 ± 1.4) and reef rock, sand, and rubble combined made up 39.4% ± 7.7% and 38.8% ± 6.8% of the benthic cover at 3 m and 10 m, respectively (Table 3). The bottom of the lagoon is mud and the depth below which there is no coral along the lagoon walls ranged from 11 m to 15 m and averaged 12.7 m. We estimate that approximately 30% of the bottom of the lagoon has no coral based on the extent of live coral shown in Fig. 1C. Assuming that half of the remaining 70% of the lagoon with coral has the same cover as the 3 m transects (22%), and the other half has the same cover as the 10 m transects (53%), this gives an average coral cover of approximately 26% for the entire lagoon.

Table 3. Average percent coverage ± standard error of major coral reef ecological categories at 3 m and 10 m in Risong Lagoon.

Major category	Average 3 m	Average 10 m
Hard coral	22.4 ± 3.9	53.0 ± 2.3
Soft coral	0	0
Other invertebrates*	3.0 ± 0.6	1.1 ± 0.7
Macroalgae	5.7 ± 2.2	0
Seagrass	0	0
Turf algae	25.6 ± 4.7	2.8 ± 1.4
Branching coralline algae	0	0
Crustose coralline algae	3.9 ± 1.4	4.2 ± 2.0
Fleshy coralline algae	0	0.1 ± 0.1
Chrysophyte	0	0
Reef rock	11.3 ± 1.4	17.2 ± 1.7
Sand	14.8 ± 2.4	13.3 ± 3.4
Rubble	13.4 ± 3.9	8.3 ± 1.7

* Includes anenomes, ascidians, sponges, *Discosoma*, gorgonians, and zoanthids.

Discussion

On Palau, coral communities inhabiting the semi-enclosed Rock Island lagoons experience levels of chronic ocean acidification equivalent to those projected for the

western tropical Pacific by the end of this century. Yet, benthic communities within these low pH lagoons appear healthy by several ecological and physiological measures, including genus richness, coral cover, coralline algal abundance, and the calcification rates of two massive coral genera (Shamberger et al. 2014; Barkley et al. 2015). To evaluate ecosystem metabolism, we quantified NEC and NEP in Risong Lagoon over two 4 d periods in the spring (March) of 2012 and the fall (November) of 2013. This is the first estimate of the whole ecosystem metabolism of a naturally low pH coral reef community. Because lagoon morphology makes the application of conventional alkalinity anomaly techniques challenging, we developed two new methods to estimate coral reef NEC and NEP in a semi-enclosed lagoon using a combination of TA, salinity, and volume budgets.

Short term perturbations – impact of typhoon Haiyan

Risong Bay surface water is the source water for Risong Lagoon (Fig. 1) and once bay surface water enters the lagoon, it is altered by coral reef ecosystem metabolism over a residence time of approximately 7 (spring tides) to 14 (neap tides) days. Thus, it takes 1–2 weeks for the lagoon to reach a steady state in which the metabolism driven flux of TA and DIC within the lagoon is balanced by advection of bay and lagoon surface water through the channel. During steady state, carbonate chemistry time trends within the lagoon are small and there is a consistent offset in carbonate chemistry between the bay and lagoon. Any perturbation to the system that disrupts this equilibrium will be immediately reflected in changes in the time trend within the lagoon that, over 1–2 weeks, will be balanced by the advective flux between the bay and lagoon until the system reaches steady state. Therefore, a careful characterization of water chemistry and circulation allows us not only to determine NEC and NEP rates, but also to evaluate whether the lagoon is in steady state or has recently experienced an environmental disturbance.

The significant TA time trend term in November 2013 (Table 2), indicates a recent (within $\sim$ 1–2 weeks) perturbation to the Risong Lagoon system. Immediately preceding the 2013 field deployment, on 06 November 2013, super typhoon Haiyan, a category 5 typhoon, passed over the northernmost islands of Palau with wind speeds over 19 m s^{-1} measured at the Koror airport. In anticipation of this event, water samples and salinity and temperature profiles were collected in Risong bay and lagoon on 05 November 2013. Samples collected before (05 November) and after (08–11 November) the typhoon reveal changes to the Risong system, including decreases in temperature and salinity of approximately 0.5°C and slightly more than 0.1, respectively, down to $\sim$ 15 m depth in both the bay and lagoon. Freshwater transport into the lagoon during the typhoon, estimated from the decrease in salinity, is equivalent to approximately 7 cm of rainfall, which agrees well with the 7.4 cm of rainfall recorded at Koror Airport from 06 November to 07 November. This freshwater input would cause a decrease in lagoon TA of about 10 μmol kg^{-1}, however, TA did not change at 1 m in the bay and TA increased by 15–20 μmol kg^{-1} at 1 m in the lagoon. There are five mechanisms by which lagoon TA could increase during the typhoon. (1) Increased advection of bay surface water, which has higher TA than lagoon surface water, into the lagoon via an increase in sea level and possibly wind forcing in the bay. (2) Vertical mixing within the lagoon. This mechanism assumes that lagoon bottom water had higher TA than lagoon surface water prior to the typhoon and that lagoon bottom water TA was close to bay surface water values. Decreases in temperature and salinity provide evidence that there was some vertical mixing, down to approximately 15 m, in both the bay and lagoon. (3) A decrease in NEC due to light limitation from increased cloud cover and/or decreased temperature. (4) Enhanced SGD. However, sea level was higher during the typhoon, in which case lagoon water should have been forced into the karst surrounding the lagoon, rather than SGD increasing. (5) Last, enhanced sediment pore water flux into the overlying water column could increase lagoon TA. While sediment pore water TA in the lagoon is elevated compared to the overlying water column (average pore water TA from 15 cm to 30 cm depth in the sediments - TA of the overlying water column = 40 ± 30 μmol kg^{-1}) and increased TA flux from the sediments is possible, the lagoon is extremely protected and it is unlikely that near-bottom water flow was significantly enhanced during the typhoon. Nevertheless, our calculations indicate that (1) or (2) alone cannot account for the entire observed TA increase in the lagoon. If (3) lagoon NEC was zero during the typhoon, TA would increase by approximately 6 μmol kg^{-1} d^{-1} and this TA flux would increase if NEC was negative during the typhoon. Some combination of 1–3 could easily explain the 15–20 μmol kg^{-1} increase in lagoon TA as well as compensate for the $\sim$ 10 μmol kg^{-1} decrease in TA expected from precipitation during the typhoon. Similarly, the source water to Risong Bay has higher TA than bay surface water and the stable bay surface water TA before and after the typhoon is likely due to these same mechanisms balancing a precipitation driven decrease in TA.

The large time trend term during our 4 d November 2013 metabolism study indicates that the system was beginning to adjust back to equilibrium immediate following the typhoon. We can estimate NEC before the typhoon by assuming that the lagoon was in steady state, so that the TA time trend was small, and by using the 1 m bay and lagoon TA data collected before the typhoon with the lower layer estimate. Salinity profiles before the typhoon show that the fresher surface layer in the lagoon was less than 1 m deep, therefore, we assume 1 m lagoon samples exclude freshwater input and are representative of lower layer lagoon carbonate chemistry before the typhoon. We estimate a pre-typhoon

NEC of 35–40 mmol m^{-2} d^{-1}, which agrees well with the post-typhoon estimate of 31–40 mmol m^{-2} d^{-1}. It is possible that NEC in the lagoon was reduced during the typhoon, presumably due to light limitation and/or decreased temperature, but our data indicate that this significant event had little effect on the NEC rate of the lagoon just days later. In contrast to more exposed reefs that can be devastated by the damage caused by strong storms, there is no indication that the coral reef system in this extremely protected lagoon was impacted by super typhoon Haiyan.

Uncertainties in NEP estimates

While there is excellent agreement between the total volume and lower layer NEC estimates for both study periods, adding confidence to these results, NEP total volume and lower layer estimates do not agree because of a large discrepancy between the advection terms in March 2012 and between the time trend terms in November 2013 (Table 2). The NEC and NEP advection terms depend on the difference between bay and lagoon carbonate chemistry, calculated either by tracking the exchange of bay and lagoon surface water through the channel with the tides (total volume calculations) or by taking the difference between bay surface water and lagoon lower layer carbonate chemistry (lower layer calculations). While there is a consistent difference between bay and lagoon TA, and therefore a consistent NEC advective flux for both total volume and lower layer calculations over both study periods, the same is not true for DIC. There is not a significant difference between bay and lagoon DIC during either study period (Fig. 4), which suggests that the NEP advection terms should be small. The large 2012 total volume advection term and the relatively large 2013 advection terms (Table 2) are likely an artifact of significant DIC diel cycles which, unlike TA, means that daytime DIC data collected in the bay and lagoon are not representative of the DIC diel averages (Fig. 4). Thus, combining daytime bay and lagoon DIC data with channel data collected throughout the diel cycle becomes problematic and biases the NEP advection terms.

The discrepancy in the 2013 NEP time trend terms is due to the fact that the 10 m lagoon DIC data, collected only in 2013, show no trend over time in contrast to the 1 m and 3 m data that show decreasing trends of similar magnitude for both study periods. Calculating the time trend terms using only 1 m and 3 m data for both years removes this discrepancy. However and importantly, the DIC time trend terms are not significantly different from zero and have low correlations ($\leq$ 0.4) between DIC and time. Therefore, NEP cannot be estimated with an acceptable level of confidence because of the large uncertainties associated with both the advection and time trend terms. Previous analyses indicated that Risong Lagoon is likely a net respiring system (Shamberger et al. 2014), in agreement with the negative 2012 lower layer and both 2013 NEP estimates in this study. Nonetheless, we cannot determine from our data whether NEP is significantly different from zero, or assess whether there is a difference in NEP that may correspond with the large difference in NEC between our two study periods.

March 2012 vs. November 2013

We measured a twofold increase in NEC between the first deployment in 2012 and the second in 2013. Environmental conditions in Risong Lagoon were similar during the two 4 d metabolism studies and cannot, on their own, explain the increase. Nor do we know the time scale over which the NEC shift occurred or on what timescales NEC varies naturally within Risong Lagoon (e.g., weeks, months, seasonal). There was no statistical difference in bay or lagoon water temperature or salinity between the two studies (Table 1). Although light levels were not measured in situ in 2012, Moderate Resolution Imaging Spectroradiometer (MODIS) measurements from the Aqua and Terra satellites (accessed at https://ladsweb.modaps.eosdis.nasa.gov) indicate cloud cover and cloud thickness were greater during the 2013 study, despite higher NEC values during this period. In addition, there was no statistical difference in bay or lagoon Ω_{ar} or pH (Table 1) and concentrations of nitrate, ammonium, and phosphate were low ($\leq$ 0.5 μM, 0.5 μM, 0.1 μM on average, respectively) during both time periods. While freshwater input was enhanced immediately prior to the 2013 study, freshwater fluxes during the 4 d metabolism studies were the same during both periods (Table 2). Ecological surveys were not performed in the lagoon until 2015 but we did not observe any obvious changes in benthic cover during our field work and no bleaching was recorded. Nevertheless, it is possible that changes in calcifier cover contributed to the difference in NEC between our study periods and/or changes in dissolution rates. NEC and NEP are often tightly correlated on hourly time scales, leading some to suggest that daytime NEC is enhanced by the elevation of reef water pH and Ω_{ar} via daytime net photosynthesis (e.g., Gattuso et al. 1999; Falter et al. 2012; DeCarlo et al. 2017). However, whether NEP drives NEC on daily and longer time scales is less clear and large uncertainties in our NEP calculations preclude us from evaluating this possibility.

The increase in NEC from March 2012 to November 2013 could reflect recovery from the 2010 bleaching event that affected coral reefs throughout Palau, including the low pH bays in the Rock Islands (van Woesik et al. 2012). Coral bleaching associated with elevated sea surface temperatures began in Palau in late June 2010 and by mid-July reef habitats throughout the archipelago had experienced significant bleaching. Coral reefs within the bays of Palau's Rock Islands experienced less bleaching and mortality than patch and outer barrier reefs, but a bleaching prevalence of up to 25% was recorded for some bay reefs (van Woesik et al. 2012). Although Risong Lagoon was not included in the coral reef surveys performed at that time, stress bands that correspond

with the 2010 bleaching event have been observed in coral skeletal cores from the lagoon and indicate that bleaching occurred (Barkley and Cohen 2016). Coral bleaching has been shown to decrease NEC (DeCarlo et al. 2017) and calcification rates of *Porites* corals can take 3–4 yr to recover post-bleaching (Cantin and Lough 2014). It is therefore feasible that the increase in Risong Lagoon NEC from 2012 to 2013 was driven by the recovery of the reef ecosystem from the 2010 bleaching event, though we do not have data to support or reject this hypothesis. While the cause of the twofold increase in NEC from March 2012 to November 2013 remains uncertain, our observations demonstrate that daily NEC rates can change dramatically within a short time frame. Marked changes in NEC rates over short periods of time, independent of changes in the environmental parameters considered the major drivers of NEC, highlight the need for repeat NEC measurements to both characterize means and variability, and understand the mechanisms underlying that variability.

Low NEC in Risong Lagoon

While Risong Lagoon maintains positive NEC rates and is therefore a net calcifying system, rates for both study periods are low compared with those measured for other coral reef systems. Few reefs with comparable calcifier cover have comparably low NEC rates (*see* Table 3 in DeCarlo et al. (2017) for a compilation of coral reef net daily NEC rates). Our data do not allow us to separate NEC into calcification vs. dissolution components, and data obtained from coral skeletal cores do not clearly point to one or the other as the driver of low NEC rates in Risong Lagoon. Calcification rates of *Porites* corals in Risong Lagoon range from approximately 0.6 to 2.1 g cm^{-2} yr^{-1}, consistent with rates reported for other Indo-Pacific reefs ($\sim$ 0.5–2.6 g cm^{-2} yr^{-1}; Lough and Cantin 2014). Bioerosion rates of *Porites* colonies, while higher than those measured on other low nutrient reefs, are not anomalously high on a global scale (DeCarlo et al. 2015). Nevertheless, while *Porites* is a dominant species on Palauan reefs, its calcification and bioerosion rates may not be representative of all calcifiers in Risong Lagoon's coral reef community. Furthermore, bioerosion rates of corals, while potentially indicative of, are not the same as reef scale dissolution rates, and there may be many sources of dissolution occurring in Risong Lagoon. For example, elevated pore water TA indicates that dissolution is also occurring within the carbonate sediments in Risong Lagoon, though our calculations show the flux of TA from the sediments into the overlying water column is at least an order of magnitude lower than NEC rates. We cannot account for all sources of dissolution individually, such as dissolution associated with microbioerosion (e.g., Tribollet et al. 2006, 2009), and while macrobioerosion rates are relatively high compared to low nutrient reefs, it remains unclear whether total dissolution is high in Risong Lagoon compared to other coral reef systems.

Whether driven by low calcification rates, high dissolution rates, or a combination of both, the environmental driver(s) of low NEC in Risong Lagoon remain unclear. In addition to chronically low pH and Ω_{ar}, Risong Lagoon is characterized by low light and low flow, both of which can depress calcification rates (Langdon and Atkinson 2005). Steep cliffs surround the lagoon and cast shade over different areas of the reef where corals grow during different times of the day, depending on the angle of the sun and the surrounding topography. Our measurements show PAR can be two orders of magnitude lower in the shade than in areas receiving direct sunlight and corals that extend down the reef slope receive less light than those near the surface. In addition, current velocities, while significant in the channel, are very low within the protected lagoon where the corals grow. There is evidence supporting a link between calcification rates and flow, possibly due to the creation of thick diffusive boundary layers under low flow conditions that restrict the flux of ions needed for calcification (Atkinson et al. 1994; Lesser et al. 1994; Langdon and Atkinson 2005). It is not possible with our existing data to determine which combination of factors are important in driving low NEC rates in Risong Lagoon. It is unclear whether calcification rates are low, dissolution rates are high, or a combination of both. Low pH, low light, and low flow conditions are all implicated in low calcification rates, and elevated bioerosion could drive higher dissolution rates. Other factors, such as community composition, including the low abundance of calcifying algae, may also play a role. Gaining a better understanding of the relative contributions of calcification vs. dissolution, and the role of different environmental and ecological parameters, is critical to predicting the future of the Risong Lagoon coral reef community and others like it. Small changes in lagoon pH, light levels, flow, or a combination of these factors could drive the system to net dissolution.

Conclusions

Rates of Net Ecosystem Calcification in the naturally low-pH Risong Lagoon are low compared to other coral reefs worldwide, despite high coral cover and diverse coral communities that inhabit the lagoon. While the chronically low pH environment in Risong Lagoon is likely contributing to low NEC rates, possibly depressing calcification and enhancing dissolution, low light and low flow likely play a role. Other factors may also be important as the twofold increase in NEC between our two study periods occurred in the absence of significant changes in temperature, salinity, inorganic nutrients, or pH. In addition, super typhoon Haiyan appears to have had no effect on the NEC of this highly protected lagoon. Repeat NEC studies on coral reefs under a variety of environmental conditions are necessary to elucidate the drivers of NEC and to ensure accurate predictions of coral reef futures under ocean acidification and other environmental changes.

References

Albright, R., C. Langdon, and K. Anthony. 2013. Dynamics of seawater carbonate chemistry, production, and calcification of a coral reef flat, central Great Barrier Reef. Biogeosciences **10**: 6747. doi:10.5194/bg-10-6747-2013

Albright, R., and others. 2016. Reversal of ocean acidification enhances net coral reef calcification. Nature **531**: 362–365. doi:10.1038/nature17155

Andersson, A., I. Kuffner, F. Mackenzie, P. Jokiel, K. Rodgers, and A. Tan. 2009. Net loss of $CaCO_3$ from a subtropical calcifying community due to seawater acidification: Mesocosm-scale experimental evidence. Biogeosciences **6**: 1811–1823. doi:10.5194/bg-6-1811-2009

Atkinson, M., E. Kotler, and P. Newton. 1994. Effects of water velocity on respiration, calcification, and ammonium uptake of a Porites compressa community. Pac. Sci. **48**: 296–303. http://hdl.handle.net/10125/2239

Barkley, H. C., A. L. Cohen, Y. Golbuu, V. R. Starczak, T. M. DeCarlo, and K. E. Shamberger. 2015. Changes in coral reef communities across a natural gradient in seawater pH. Sci. Adv. **1**: e1500328. doi:10.1126/sciadv.1500328

Barkley, H. C., and A. L. Cohen. 2016. Skeletal records of community-level bleaching in *Porites* corals from Palau. Coral Reefs **35**: 1407–1417. doi:10.1007/s00338-016-1483-3

Barkley, H. C., A. L. Cohen, D. C. McCorkle, and Y. Golbuu. 2017. Mechanisms and thresholds for pH tolerance in Palau corals. J. Exp. Mar. Biol. Ecol. **489**: 7–14. doi:10.1016/j.jembe.2017.01.003

Bernstein, W., K. Hughen, C. Langdon, D. McCorkle, and S. Lentz. 2016. Environmental controls on daytime net community calcification on a Red Sea reef flat. Coral Reefs **35**: 697–711. doi:10.1007/s00338-015-1396-6

Cantin, N. E., and J. M. Lough. 2014. Surviving coral bleaching events: *Porites* growth anomalies on the Great Barrier Reef. PLoS ONE **9**: e88720. doi:10.1371/journal.pone.0088720

Costanza, R., R. S. de Groot, P. Sutton, S. van der Ploeg, S. J. Anderson, I. Kubiszewski, S. Farber, and R. K. Turner. 2014. Changes in the global value of ecosystem services. Glob. Environ. Change **26**: 152–158. doi:10.1016/j.gloenvcha.2014.04.002

Crook, E., D. Potts, M. Rebolledo-Vieyra, L. Hernandez, and A. Paytan. 2012. Calcifying coral abundance near low-pH springs: Implications for future ocean acidification. Coral Reefs **31**: 239–245. doi:10.1007/s00338-011-0839-y

Crook, E. D., A. L. Cohen, M. Rebolledo-Vieyra, L. Hernandez, and A. Paytan. 2013. Reduced calcification and lack of acclimatization by coral colonies growing in areas of persistent natural acidification. Proc. Natl. Acad. Sci. USA **110**: 11044–11049. doi:10.1073/pnas.1301589110

DeCarlo, T. M., A. L. Cohen, H. C. Barkley, Q. Cobban, C. Young, K. E. Shamberger, R. E. Brainard, and Y. Golbuu. 2015. Coral macrobioerosion is accelerated by ocean acidification and nutrients. Geology **43**: 7–10. doi:10.1130/G36147.1

DeCarlo, T. M., A. L. Cohen, G. T. F. Wong, F.-K. Shiah, S. J. Lentz, K. A. Davis, K. E. F. Shamberger, and G. P. Lohmann. 2017. Community production modulates coral reef pH and the sensitivity of ecosystem calcification to ocean acidification. J. Geophys. Res. Oceans **122**: 745–761. doi:10.1002/2016JC012326

Dickson, A., and F. J. Millero. 1987. A comparison of the equilibrium constants for the dissociation of carbonic acid in seawater media. Deep-Sea Res. Part A Oceanogr. Res. Pap. **34**: 1733–1743. doi:10.1016/0198-0149(87)90021-5

Dickson, A. G., C. L. Sabine, and J. R. Christian (Eds.). 2007. Guide to Best Practices for Ocean CO_2 Measurements. PICES Special Publication, **3**: 191 pp.

Fabricius, K. E., and others. 2011. Losers and winners in coral reefs acclimatized to elevated carbon dioxide concentrations. Nat. Clim. Chang. **1**: 165–169. doi:10.1038/nclimate1122

Falter, J. L., R. J. Lowe, M. J. Atkinson, and P. Cuet. 2012. Seasonal coupling and de-coupling of net calcification rates from coral reef metabolism and carbonate chemistry at Ningaloo Reef, Western Australia. J. Geophys. Res. Oceans **117**: C05003. doi:10.1029/2011JC007268

Gattuso, J., M. Pichon, B. Delesalle, C. Canon, and M. Frankignoulle. 1996. Carbon fluxes in coral reefs. I. Lagrangian measurement of community metabolism and resulting air-sea CO_2 disequilibrium. Mar. Ecol. Prog. Ser. **145**: 109–121. doi:10.3354/meps145109

Gattuso, J.-P., D. Allemand, and M. Frankignoulle. 1999. Photosynthesis and calcification at cellular, organismal and community levels in coral reefs: A review on interactions and control by carbonate chemistry. Am. Zool. **39**: 160–183. doi:10.1093/icb/39.1.160

Kohler, K. E., and S. M. Gill. 2006. Coral Point Count with Excel extensions (CPCe): A Visual Basic program for the determination of coral and substrate coverage using random point count methodology. Comput. Geosci. **32**: 1259–1269. doi:10.1016/j.cageo.2005.11.009

Koweek, D., R. B. Dunbar, J. S. Rogers, G. J. Williams, N. Price, D. Mucciarone, and L. Teneva. 2015. Environmental and ecological controls of coral community metabolism on Palmyra Atoll. Coral Reefs **34**: 339–351. doi:10.1007/s00338-014-1217-3

Langdon, C., and others. 2000. Effect of calcium carbonate saturation state on the calcification rate of an experimental coral reef. Global Biogeochem. Cycles **14**: 639–654. doi:10.1029/1999GB001195

Langdon, C., and others. 2003. Effect of elevated CO_2 on the community metabolism of an experimental coral reef. Global Biogeochem. Cycles **17**: 1011. doi:10.1029/2002GB001941

Langdon, C., and M. Atkinson. 2005. Effect of elevated pCO_2 on photosynthesis and calcification of corals and interactions with seasonal change in temperature/irradiance and nutrient enrichment. J. Geophys. Res. Oceans **110**. doi:10.1029/2004JC002576

Lee, K., L. T. Tong, F. J. Millero, C. L. Sabine, A. G. Dickson, C. Goyet, G.-H. Park, R. Wanninkhof, R. A. Feely, and R. M. Key. 2006. Global relationships of total alkalinity with salinity and temperature in surface waters of the world's oceans. Geophysical Research Letters **33**: 1–5. doi:10.1029/2006GL027207

Lesser, M. P., V. M. Weis, M. R. Patterson, and P. L. Jokiel. 1994. Effects of morphology and water motion on carbon delivery and productivity in the reef coral, Pocillopora damicornis (Linnaeus): Diffusion barriers, inorganic carbon limitation, and biochemical plasticity. J. Exp. Mar. Biol. Ecol. **178**: 153–179. doi:10.1016/0022-0981(94)90034-5

Lewis, E., D. Wallace, and L. J. Allison. 1998. Program developed for CO2 system calculations. Carbon Dioxide Information Analysis Center, managed by Lockheed Martin Energy Research Corporation for the US Department of Energy Tennessee.

Lough, J. M., and N. E. Cantin. 2014. Perspectives on massive coral growth rates in a changing ocean. Biol. Bull. **226**: 187–202. doi:10.1086/BBLv226n3p187

Manzello, D. P., J. A. Kleypas, D. A. Budd, C. M. Eakin, P. W. Glynn, and C. Langdon. 2008. Poorly cemented coral reefs of the eastern tropical Pacific: Possible insights into reef development in a high-CO_2 world. Proc. Natl. Acad. Sci. USA **105**: 10450–10455. doi:10.1073/pnas.0712167105

Mehrbach, C., C. H. Culberson, J. E. Hawley, and R. M. Pytkowicz. 1973. Measurement of the Apparent Dissociation Constants of Carbonic Acid in Seawater at Atmospheric-Pressure. Limnology and Oceanography **18**: 897–907.

Muehllehner, N., C. Langdon, A. Venti, and D. Kadko. 2016. Dynamics of carbonate chemistry, production, and calcification of the Florida Reef Tract (2009–2010): Evidence for seasonal dissolution. Global Biogeochem. Cycles **30**: 661–688. doi:10.1002/2015GB005327

Ohde, S., and R. van Woesik. 1999. Carbon dioxide flux and metabolic processes of a coral reef, Okinawa. Bull. Mar. Sci. **65**: 559–576.

Shamberger, K., R. A. Feely, C. L. Sabine, M. J. Atkinson, E. H. DeCarlo, F. T. Mackenzie, P. S. Drupp, and D. A. Butterfield. 2011. Calcification and organic production on a Hawaiian coral reef. Mar. Chem. **127**: 64–75. doi:10.1016/j.marchem.2011.08.003

Shamberger, K. E., A. L. Cohen, Y. Golbuu, D. C. McCorkle, S. J. Lentz, and H. C. Barkley. 2014. Diverse coral communities in naturally acidified waters of a Western Pacific reef. Geophys. Res. Lett. **41**: 499–504. doi:10.1002/2013GL058489

Shaw, E. C., B. I. McNeil, and B. Tilbrook. 2012. Impacts of ocean acidification in naturally variable coral reef flat ecosystems. J. Geophys. Res. Oceans **117**: C03038. doi:10.1029/2011JC007655

Shaw, E. C., S. R. Phinn, B. Tilbrook, and A. Steven. 2015. Natural in situ relationships suggest coral reef calcium carbonate production will decline with ocean acidification. Limnol. Oceanogr. **60**: 777–788. doi:10.1002/lno.10048

Silverman, J., B. Lazar, and J. Erez. 2007. Effect of aragonite saturation, temperature, and nutrients on the community calcification rate of a coral reef. J. Geophys. Res. Oceans **112**. doi:10.1029/2006JC003770

Silverman, J., B. Lazar, L. Cao, K. Caldeira, and J. Erez. 2009. Coral reefs may start dissolving when atmospheric CO_2 doubles. Geophys. Res. Lett. **36**: L05606. doi:10.1029/2008GL036282

Silverman, J., D. I. Kline, L. Johnson, T. Rivlin, K. Schneider, J. Erez, B. Lazar, and K. Caldeira. 2012. Carbon turnover rates in the One Tree Island reef: A 40-year perspective. J. Geophys. Res. Biogeosci. **117**: G03023. doi:10.1029/2012JG001974

Silverman, J., and others. 2014. Community calcification in Lizard Island, Great Barrier Reef: A 33year perspective. Geochim. Cosmochim. Acta **144**: 72–81. doi:10.1016/j.gca.2014.09.011

Smith, S., and G. Key. 1975. Carbon dioxide and metabolism in marine environments. Limnol. Oceanogr. **20**: 493–495. doi:10.4319/lo.1975.20.3.0493

Tribollet, A., M. J. Atkinson, and C. Langdon. 2006. Effects of elevated pCO_2 on epilithic and endolithic metabolism of reef carbonates. Glob. Chang. Biol. **12**: 2200–2208. doi:10.1029/2008GB003286

Tribollet, A., C. Godinot, M. Atkinson, and C. Langdon. 2009. Effects of elevated pCO_2 on dissolution of coral carbonates by microbial euendoliths. Global Biogeochem. Cycles **23**: G03023. doi:10.1029/2008GB003286

van Woesik, R., P. Houk, A. D. Isechal, J. W. Idechong, S. Victor, and Y. Golbuu. 2012. Climate-change refugia in the sheltered bays of Palau: Analogs of future reefs. Ecol. Evol. **2**: 2474–2484. doi:10.1002/ece3.363

Acknowledgments

The authors thank Y. Golbuu, H.C. Barkley, K. Pietro, G.P. Lohmann, D. McCorkle, R. Belastock, K. Hoering, M.E. Gonneea, A. Helbling, and the staff of the Palau International Coral Reef Center for assistance with fieldwork and analyses. We would also like to thank M.E. Gonneea for trace metal work and very helpful discussions on budgets for the lagoon. The authors thank two anonymous reviewers for valuable comments that improved the manuscript. This work was supported by NSF award 1220529 to A.L.C., S.J.L., and K.E.F.S. and a Woods Hole Oceanographic Institution Postdoctoral Scholarship to K.E.F.S.

Conflict of Interest

None declared.

Submitted 26 April 2017
Revised 26 July 2017
Accepted 27 July 2017

Associate editor: Jim Falter